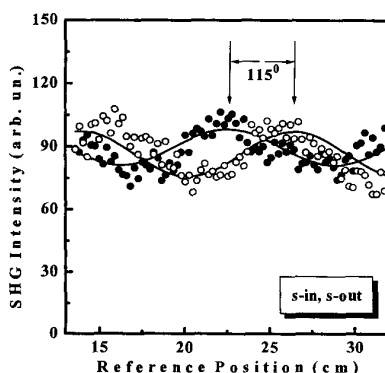


QThB8 Fig. 1. SHG scattering indicatrix for Gd LB film.

nm. A single beam SHG interferometry<sup>1</sup> is performed as indium-tin oxide being a source of a reference SHG signal. The DC-magnetic field up to 1.5 kOe is applied to the sample in the longitudinal geometry.

Figure 1 shows a typical scattering indicatrix, i.e. dependence of the SHG intensity on the angle of reflection for the fixed angle of incidence (45°) measured in p-in, p-out polarization combination of the fundamental and SH waves. Similar SHG indicatrices are observed for all the polarization combinations. The SHG radiation is scattered into a broad angular interval, that indicates an inhomogeneity of spatial distribution of nonlinear sources. This inhomogeneity should be attributed to the presence of 2D islands of Gd ions with noncentrosymmetric geometrical shape. Apart from diffuse SHG, a noticeable peak of the specular reflection is observed (inset in Fig. 1). It can appear due to the predominant in-plane orientation of these 2D Gd islands caused by the procedure of the film deposition.

The magnetoinduced effects are studied for the specular SHG component. The SHG polarization diagrams show an angular shift of 12 degrees as the DC-magnetic field of 1 kOe and of the opposite directions is applied. Figure 2 shows the results of the SHG phase measurements that reveal the magnetoinduced shift of the SH wave phase of approximately 115 de-



QThB8 Fig. 2. The SHG interference patterns from Gd-containing LB film for the longitudinal application of the DC-magnetic field in s-in, s-out polarization combination: open circles—1 kOe, filled circles—1 kOe.

grees for the s-in, s-out polarization combination, while for the p-to-p polarization combination it is less than 5 degrees. Significant magnitude of magnetization induced effects in SHG from Gd 2D layers in LB films which manifest themselves in sufficient angles of rotation of the SH wave polarization and variations of the SH wave phase indicate a strong coupling between nonmagnetic and magneto-induced nonlinear polarizations of the Gd layer.

This work was supported by INTAS Fellowship grants for Young Scientists YSF-8,10.

1. R. Stolle, G. Marowsky, E. Schwarzberg, and G. Berkovic, *Appl. Phys. B* **63**, 491 (1996).

## QThC

8:00 am–10:00 am  
Rooms 341/342

### Optical Processes in Organic Materials

Misha Y. Ivanov, *SIMS NRC, Canada, President*

#### QThC1 (Invited)

8:00 am

### Morphology-dependent photophysics in conjugated polymers

Benjamin J. Schwartz, *Chemistry Dept., UCLA 405 Hilgard Ave., Los Angeles, CA, 900095 USA; E-mail: schwartz@chem.ucla.edu*

We present evidence that the degree of interchain interactions and morphology in conjugated polymer films can be controlled by altering the chain conformation in the solution from which the film is cast. Light scattering experiments show that physical size of poly[2-methoxy-5-(2'-ethyl-hexyloxy)-1,4-phenylene vinylene] (MEH-PPV) chains can vary by a factor of two in different solvents such as chlorobenzene (CB) or tetrahydrofuran (THF). Photoluminescence and wavelength-dependent excitation indicate that MEH-PPV forms aggregate species with an absorption and luminescence spectra that are distinctly red-shifted from the intrachain exciton. The degree of aggregation is both concentration and solvent dependent; for solutions with concentrations typical of those used in spin-casting, aggregates comprise a significant fraction of the total number of excited state species. The overall photoluminescence quantum yield is found to depend on both how restricted the polymer conformation is due to choice of solvent and polymer concentration due to aggregation. The excited state aggregates have a longer lifetime than their intrachain exciton counterparts, as evidenced by a near-infrared transient absorption in femtosecond pump-probe and anisotropy measurements. Memory of the chain conformation and extent of aggregation of MEH-PPV in solution is carried into cast films. Thus, many conflicting results presented on the degree of interchain interactions can be explained by noting that the film samples in different studies were cast from precursor solutions with different solvents and concentra-

tions. Overall, careful choice of the solution (both solvent and concentration) can be used to produce MEH-PPV films with desired interchain interactions for particular device applications.

#### QThC2

8:30 am

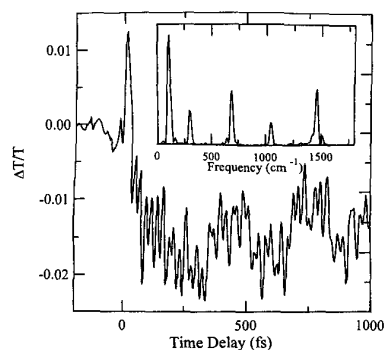
### Real time vibronic coupling dynamics in organic conjugated systems

G. Lanzani, G. Cerullo,\* S. De Silvestri,\* O. Svelto, *Istituto Nazionale per la Fisica della Materia, Istituto di Matematica e Fisica, Università di Sassari, I-07100, Sassari, Italy; E-mail: lanzani@ssmain.uniss.it*

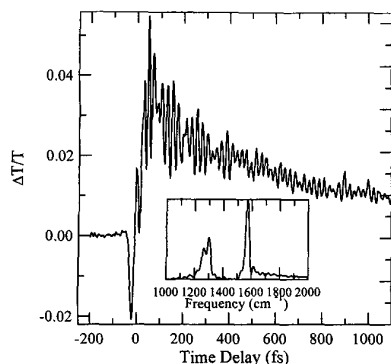
Upon electronic excitation, linear  $\pi$ -conjugated chains (both oligomers and polymers) show substantial alterations in the geometrical configuration of the carbon skeleton. Re-organization into a stable excited state may result into variations of the C-C bond length up to 5 pm. Bond-order alternation may be reduced to zero or switched, and in long chains it has been suggested that topological defects can be generated.<sup>1</sup> Two important consequences of the strong electron-phonon coupling in such systems are the presence of a Peierls distortion in the ground state and the possibly large vibronic coupling, especially in case of closely lying excited states.<sup>2</sup> For these reasons, vibrational dynamics and vibronic coupling have been the subject of extensive studies, theoretical as well as experimental. Impulsive coherent vibrational spectroscopy (ICVS)<sup>3</sup> is a recent approach to this challenge, made possible by the advent of new ultrashort laser sources (below 10 fs) which allow to monitor in real time linear chain normal modes with frequency up to 2000  $\text{cm}^{-1}$ .

In this work we show the potentialities of applying ICVS to conjugated systems relevant for applications. We studied films of sexithiophene ( $T_6$ ), a candidate for large area molecular electronics,<sup>4</sup> poly-phenylene vinylene (PPV), a prototype electroluminescent material,<sup>5</sup> and polydiacetylene (PDA), very promising for applications in photonic devices.<sup>6</sup> The experiments were performed using a novel optical parametric amplifier based on non-collinear phase matching in  $\beta$ -barium borate,<sup>7</sup> which provides pulses with bandwidths broader than 50 THz, sub-10-fs duration and tunability from 490 to 700 nm.

In Fig. 1 we show pump-probe data for  $T_6$  excited by a pulse with 520 nm center wavelength; the probe wavelength, selected with an interference filter after the sample, is 510 nm. The photoinduced absorption is strongly modulated by a complex oscillatory pattern, the Fourier transform of which is shown in the inset. Five modes are clearly identified, with frequency ranging from 110  $\text{cm}^{-1}$  to 1450  $\text{cm}^{-1}$ . These data allow a conclusive assignment of the vibronic structure in  $T_6$  and shed light on the vibronic coupling mechanism between lower excited states. By taking the Fourier transform of different time windows of the signal, we clearly observe a shift of the 1450  $\text{cm}^{-1}$  mode towards higher frequency upon increasing the time delay. This is interpreted as due to relaxation of the vibrational wavepacket within an anharmonic potential energy surface.



**QThC2 Fig. 1.** Differential transmission  $\Delta T/T$  vs. delay for a PDA film pumped with a center wavelength of 520 nm and probed at 510 nm. The inset shows the Fourier transform of the oscillatory component of the signal.

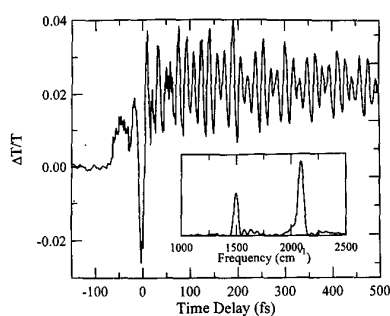


**QThC2 Fig. 2.** Differential transmission  $\Delta T/T$  vs. delay for a PPV film pumped with a center wavelength of 540 nm and probed at 590 nm. The inset shows the Fourier transform of the oscillatory component of the signal.

An example of the results obtained in PPV in the stimulated emission (SE) region (pump at 540 nm and probe at 590 nm) is given in Fig. 2. The Fourier transform indicates the presence of two strongly coupled modes, assigned to the transvinylene C-C stretching (at  $1290\text{ cm}^{-1}$ ) and ring quadrant C-C stretching (at  $1570\text{ cm}^{-1}$ ) respectively. In PDA the SE signal (pump at 540 nm, probe at 610 nm), shown in Fig. 3, is not instantaneous, pointing to a thermalization process which is completed in about 100 fs. For the first time we observe real time oscillations above 2000 wavenumbers, corresponding to the triple carbon bond stretching mode of PDA. The data allow to investigate the geometrical configuration of the excited state, which is expected to have a substantial contribution of butatrienic character. Time evolution of the vibrational frequency is discussed in view of the existing theoretical models.

In conclusion, these experiments demonstrate the possibility of studying coherent molecular dynamics in organic systems with extremely high time resolution.

*\*Istituto Nazionale Fisica della Materia, CEQSE-CNR, Dipartimento di Fisica, Politecnico, I-20133 Milano, Italy*



**QThC2 Fig. 3.** Differential transmission  $\Delta T/T$  vs. delay for a PDA film pumped with a center wavelength of 540 nm and probed at 610 nm. The inset shows the Fourier transform of the oscillatory component of the signal.

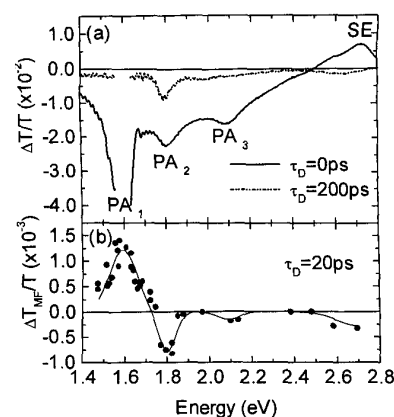
1. A.J. Heeger, S. Kivelson, J.R. Schrieffer, and W.P. Su, *Rev. Mod. Phys.* **60**, 781 (1988).
2. E. Ehrenfreund, Z. Vardeny, O. Brafman, and B. Horowitz, *Phys. Rev. B* **36**, 1535 (1987); G. Orlandi, F. Zerbetto, *Chem. Phys.* **108**, 187 (1986).
3. S. Mukamel, *Principles of nonlinear optical spectroscopy*, Oxford University Press, New York, 1995.
4. C. Ziegler, in *Handbook of Conductive Molecules and Polymers*, edited by H.S. Nalwa (Wiley, New York, 1997), Vol. 3, p. 676.
5. J.H. Burroughes, D.D.C. Bradley, A.R. Brown, R.N. Marks, K. Mackay, R.H. Friend, P.L. Burn, A. Kraft, A.B. Holmes, *Nature* **347**, 539 (1990).
6. *Relaxation in Polymers*, edited by T. Kobayashi (World Scientific, Singapore, 1993).
7. G. Cerullo, M. Nisoli, and S. De Silvestri, *Appl. Phys. Lett.* **71**, 3616 (1997); G. Cerullo, M. Nisoli, S. Stagira, and S. De Silvestri, *Opt. Lett.* **23**, 1283 (1998).

### QThC3 8:45 am

#### Photogeneration of triplet states by polaron recombination in para-hexaphenyl

C. Zenz,\* G. Cerullo,\*\* G. Lanzani, W. Graupner,† F. Meghdadi,† G. Leising,† S. De Silvestri,\*\* *Istituto Nazionale per la Fisica della Materia, Istituto di Matematica e Fisica, Università di Sassari, Via Vienna 2, I-07100, Sassari, Italy; E-mail: f513zenz@mbox.tu-graz.ac.at*

Dissociation of photo-generated excitons into charge carriers (polarons) is the working principle of organic photovoltaic cells, whereas recombination of field-injected charge carriers into luminescent singlet excitons and non-radiative triplet excitons governs the efficiency of organic light emitting devices (OLED). In this paper, we address these processes in a single layer OLED based on para-hexaphenyl (PHP)<sup>1</sup> by conventional and electric field-assisted femtosecond pump/probe measurements. Due to its well defined conjugation length and its chemical structure PHP exhibits well resolved photo-induced absorption (PA)



**QThC3 Fig. 1.** (a) Conventional transient pump/probe spectra of the polycrystalline PHP film for different pump-probe delays ( $\tau_D$ ), measured in an OLED-structure. (b) Field-induced  $(\Delta T/T)_{MF}$ -spectrum of PHP films for pump-probe delay of 20 ps and an applied reverse bias of 16 V. Data points are obtained using a monochromator or interference filters. The solid line is a guide to the eye.

features, that can be assigned to singlet, triplet and polaron absorption. This allows to monitor the dynamics of field-induced singlet dissociation<sup>2</sup> and polaron recombination in a single layer OLED structure consisting of aluminum/PHP/Indium Tin Oxide (ITO) with 200 fs time resolution.

Figure 1(a) shows conventional differential transmission spectra for 0 ps and 200 ps pump-probe delays ( $\tau_D$ ). We observe three PA-bands peaking at 1.59 eV ( $PA_1$ ), 1.8 eV ( $PA_2$ ), and 2.09 eV ( $PA_3$ ), and a strong stimulated emission (SE) band for probe energies higher than 2.5 eV. The field-induced changes of PA under the same experimental conditions for an applied reverse bias of 16 V and a pump-probe delay of 20 ps are depicted in Fig. 1(b). From this spectrum, a field-induced quenching of SE and  $PA_1$  is evident, whereas both  $PA_2$  and  $PA_3$  are increased.

$PA_1$  is assigned to singlet exciton absorption due to the correspondence with SE-dynamics<sup>3</sup> and the field-induced quenching by exciton dissociation.  $PA_3$  at 2.09 eV can be assigned to polaron absorption as indicated by theoretical calculations and comparison with doping induced measurements. This assignment is also supported by the observed field-induced increase of  $PA_3$ .

The absorption band at 1.8 eV ( $PA_2$ ) has been assigned to triplet absorption being the only persistent spectral feature for pump-probe delays longer than 200 ps [see Fig. 1(a)] and based on comparison with cw-PA measurements.<sup>4</sup> The differential transmittance spectrum at 0 ps delay, that already contains this feature, suggests a triplet exciton formation within the pump pulse ( $\tau_p < 200$  fs). Due to the observed dynamics and the energetic position of the pump, we exclude intersystem crossing (ISC) and singlet fission to be the dominant triplet generation mechanism under these experimental conditions. More insight into the triplet formation can be gained by studying the dynamics of the field-induced